Available online at www.sciencedirect.com
ScienceDirect
Journal of Power Sources 178 (2008) 97–102
JOURNAL OF POWER SOURCES
www.elsevier.com/locate/jpowsour

Short communication

Role of structural H_2O in TiO_2 nanotubes in enhancing Pt/C direct ethanol fuel cell anode electro-catalysts

Huanqiao Song [a], Xinping Qiu [b,*], Daojun Guo [b], Fushen Li [a]

[a] *School of Materials Science and Engineering, University of Science and Technology Beijing, Beijing 100083, China*
[b] *Key Lab of Organic Optoelectronics and Molecular Engineering, Department of Chemistry, Tsinghua University, Beijing 100084, China*

Received 22 September 2007; received in revised form 1 November 2007; accepted 5 November 2007
Available online 22 November 2007

Abstract

TiO_2 nanotubes (TNTs) with different structural water were obtained by heat treatment under different temperatures. The role of the structural water in TNTs co-catalyzing ethanol oxidation with Pt/C catalyst was studied systematically. Electrochemical studies using cyclic voltammetry and CO stripping voltammetry indicated that more structural water in TNTs was favorable for improving the tolerance of Pt/C to poisoning species; while chronoamperometry curves and repeated cyclic voltammograms showed that slightly less structural water in TNTs actually led to higher catalytic activity and better stability of Pt/C catalysts for ethanol oxidation. This strange result has been analyzed and was ascribed to the appropriate balance of bi-functional mechanism and ethanol transfer in the catalyst layer with less structural water.

Keywords: Electro-catalysts; Structural water; Titanium oxide nanotube; Catalyst layer; Ethanol electro-oxidation

1. Introduction

By far, platinum is still the most promising catalyst for the oxidation of alcohol in direct alcohol fuel cell (DAFC). Its superior catalytic activity, however, drops severely with time during the alcohol oxidation because of the presence of CO-like intermediate species. These poisoning species are not oxidized away unless the anode potential is increased to greater than 0.6 V (RHE), where OH adsorption (OH_{ad}) allows the poisoning species to oxidize via a Langmuir–Hinshelwood type surface reaction between the poisoning species and OH_{ad}. The net result of this increase in potential is an unacceptable loss of cell voltage and efficiency [1]. To solve this problem, lots of work has been done [2–6] and the most widely accepted strategy is to use Pt-based alloys or Pt/metal oxide composites, relying on the bi-functional mechanism [7] and the electronic effect [8] to reduce the potential of CO-like species oxidation or weaken its absorption on Pt. Recently, more and more work has been focused on the system of Pt/transition metal oxide composites, such as Pt–CeO_2 [9], Pt–TiO_2 [10] and Pt–SnO_2 [11]; and some excellent results have been presented. However, there have been few studies on how the catalytic activities of these catalysts are increased.

Titania nanotubes (TNTs) – TiO_2 with special tube-like structure – have great potential as a material with novel properties that are not found in conventional TiO_2. It has been proved that they have larger surface area and higher photocatalytic activity than TiO_2 [12]; and as a support of Pd, it has presented excellent catalytic activity for methanol oxidation in acid solution [13]. In a recent study, we have found that TNTs exhibited wonderful co-catalyzing effect together with Pt for ethanol electro-oxidation [14]: the current density was improved by about 87% and the onset potential of ethanol oxidation shifted negatively for about 0.1 V compared with Pt/C catalysts. The possible reason for the increased catalytic activity was ascribed to the abundant structural water contained in TNTs. However, the exact mechanism through which the structural water affected the activity of the catalysts was unknown, and further research on the role of structural water in ethanol electro-oxidation was needed.

In the present study, the role of structural water in ethanol electro-oxidation was investigated in detail by performing cyclic voltammetry (CV), chronoamperometry and CO stripping

* Corresponding author. Tel.: +86 10 62794234; fax: +86 10 62794234.
E-mail address: qiuxp@mail.tsinghua.edu.cn (X. Qiu).

0378-7753/$ – see front matter © 2007 Elsevier B.V. All rights reserved.
doi:10.1016/j.jpowsour.2007.11.044

voltammetry on Pt/C + TNTs with various amount of structural water. These data are critical to the further understanding of the mechanism of ethanol electro-oxidation as well as to the development of new low-cost direct ethanol (or alcohol) fuel cell anode catalysts.

2. Experimental

Titanium dioxide powders were first prepared using the sol–gel method [15]. Afterwards, the as-prepared anatase titanium dioxide powders were put into a 250 mL Nalgene flask with 100 mL of 10 M sodium hydroxide aqueous solution to create TNTs. The flask was maintained at 110 °C for 24 h in an oil bath. The treated powders were then washed thoroughly with 0.1 M hydrochloric acid aqueous solution and distilled water; and subsequently separated from the washing solution by centrifugation. This operation was repeated until the pH value of the washing water was under 7. After drying in vacuum at 80 °C for 5 h [16,17], the precipitates were divided into four batches. No further heat treatment was performed on the first batch. The second, third and fourth batches were heated at 200, 300 and 400 °C, respectively for 2 h. These samples were named TNT-R, TNT-200, TNT-300 and TNT-400, reflecting their respective heating temperature.

Thermal gravity analysis (TGA) was performed using a Universal V5.3C 2050 Instrument in the temperature range of room temperature to 800 °C at a scanning rate of 10 °C min^{-1}. X-ray diffraction (XRD) analysis was performed using a Rigaku X-ray diffractometer with Cu Kα-source. The 2θ angular regions between 20° and 90° were studied at a scan rate of 6° min^{-1} with a step of 0.02°. The surface morphology of the catalysts was observed on a scanning electron microscope (SEM, JSM-6301F) with an energy-dispersive X-ray (OXFORD INCA 300). The BET surface area of each catalyst was determined by means of nitrogen physisorption, using a Quantachrome NOVA automated gas sorption instrument.

The catalyst slurry containing 16.6% the prepared TNTs and 83.4% Pt/C (E-TEK; 20 wt.% Pt on Vulcan) was deposited on a gold electrode (1 cm × 1 cm) to determine the ethanol oxidation activity. It means that the weight ratio of TNT to Pt was close to 1:1. The catalyst slurry was prepared by mixing Pt/C with TNT-X (X = R, 300 and 400) in distilled water under sonication for 30 min, and then adding Nafion (20% Nafion and 80% ethylene glycol) solution for another 10 min. After casting, the catalysts were air-dried for 60 min at 80 °C. These dried catalysts were denoted as Pt/C + TNT-X (X = R, 300 and 400). The normal loading of the catalysts on the gold electrode was 1 mg cm^{-2}. Electrochemical measurements were carried out in a three electrode cell using a Solartron workstation at 25 °C. The gold patch coated with catalyst ink was used as the working electrode. A saturated calomel electrode (SCE) and Pt gauze were used as the reference and the counter electrodes, respectively. The reference electrode was connected to the electrochemical cell by a KNO_3 salt bridge to avoid contamination of Cl^- anion. All electrode potentials in this paper are referred to the SCE. A solution of 1 M $HClO_4$ or 1 M C_2H_5OH + 1 M $HClO_4$ was used as the electrolyte. All the reagents used were of analytical grade. The activation scans were performed until reproducible voltammograms were obtained. Cyclic voltammograms were recorded in the potential range of −0.2 to 1 V versus SCE at a scan rate of 50 mV s^{-1}. The chronoamperometric curves were recorded at 0.45 V for 3600 s. The oxidation of pre-adsorbed carbon monoxide (CO) was measured by CO stripping voltammetry in 1 M $HClO_4$ solution at a scan rate of 10 mV s^{-1}.

3. Results and discussion

Fig. 1 shows the TGA curves for TNT-R, TNT-200, TNT-300 and TNT-400. It can be seen that the amount of structural water in TNTs reduced as the heat treatment temperature increased. Though there was almost no change before 200 °C, only half of the structural water remained after the heat treatment at 300 °C, and the TNTs were dehydrated completely when the heating temperature reached 400 °C. This result shows that the structural water in TNTs was more stable at the lower temperatures, though it could be removed completely at high temperatures. Further study on TNT-400 (not shown) after exposed to air for 10 days proved that once the structural water escaped, it could not be reintroduced.

The XRD patterns of TNT-R, TNT-300, TNT-400 and anatase TiO_2 are shown in Fig. 2. Comparing the four samples, it can be easily seen that all the peaks correspond to the anatase structure of the TiO_2. The height and the width of the diffraction peaks for TNT-R, TNT-300 and TNT-400 were almost the same, suggesting that the structure of the TNTs was stable and that the TNT-R particles did not grow with the increase of heating temperature.

For the rest of the paper, we will use TNT-R, TNT-300 and TNT-400 as the bases of our discussion on the effect of structural water on the catalytic activity of Pt/C catalysts.

The electrochemical performances of Pt/C + TNT-X (X = R, 300 and 400) were tested for ethanol oxidation. As shown in Fig. 3, the CV curves of ethanol oxidation at the water-containing Pt/C + TNT-R and Pt/C + TNT-300 were very similar to that of Pt/C + TNT-400, which has no water. In the forward scan, ethanol oxidation produced a prominent symmetric anodic peak around 0.80 V. The data for the three catalysts are listed

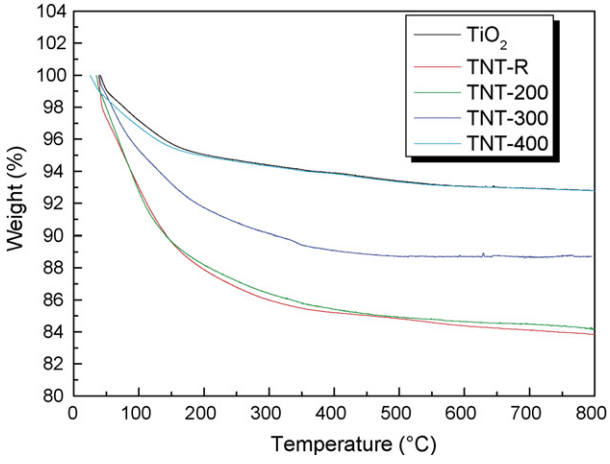

Fig. 1. TGA curves of anatase TiO_2 and TiO_2 nanotubes (TNT-X) within the temperature range of room temperature to 800 °C.

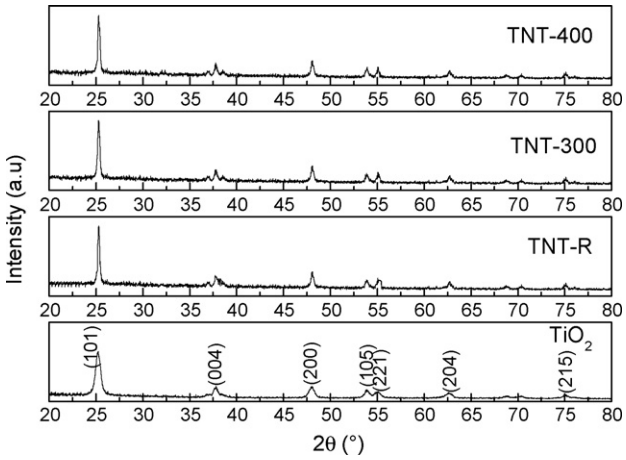

Fig. 2. XRD patterns of TNT-R, TNT-300, TNT-400 and anatase TiO_2.

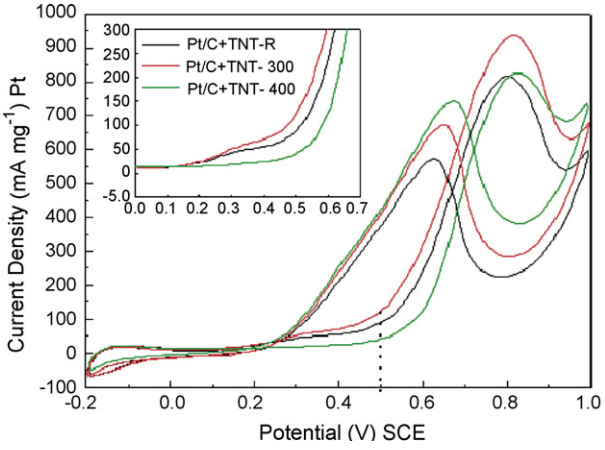

Fig. 3. Cyclic voltammogram curves for ethanol electro-oxidation at Pt/C + TNT-R, Pt/C + TNT-300 and Pt/C + TNT-400 electrode in 1 M C_2H_5OH + 1 M $HClO_4$ solutions with a scan rate of 50 mV s^{-1}.

in Table 1. They show that Pt/C + TNT-R and Pt/C + TNT-300 had lower peak potentials than Pt/C + TNT-400. In addition, the higher current densities (at the same potential, e.g. 0.5 V) at the Pt/C + TNT-R and Pt/C + TNT-300 electrodes also suggest their higher catalytic activities for ethanol oxidation. In the reverse scan, an oxidation peak was observed around 0.64 V. This peak is usually considered to be associated with the removal of the carbonaceous species generated via incomplete oxidation of alcohol in the forward scan [18–23]. These carbonaceous species included absorbed CH_3CO, absorbed CO and CH_3CHO species in ethanol oxidation [24,25], which could be oxidized according to the following reaction:

$$\text{Pt–CO–CH}_3 + \text{Pt–OH} \rightarrow 2\text{Pt} + \text{CH}_3\text{–COOH} \quad (1)$$

or

$$\text{Pt–CO–CH}_3 + \text{Pt} \rightarrow \text{Pt–CO} + \text{Pt–CH}_3 \quad (2)$$

$$\text{Pt–CO} + \text{Pt–OH} \rightarrow \text{CO}_2 + 2\text{Pt} + \text{H}^+ + \text{e}^- \quad (3)$$

$$\text{CHO–CH}_3 + \text{Pt–OH} \rightarrow \text{Pt} + \text{CH}_3\text{–COOH} + \text{H}^+ + \text{e}^- \quad (4)$$

Hence the ratio of the forward oxidation peak current density (I_f) to the reverse peak current density (I_b), I_f/I_b, can be used to describe the catalyst tolerance to the poisoning species. A higher I_f/I_b ratio indicates more effective removal of the poisoning species on the catalyst surface. In Fig. 3, the I_f/I_b ratios of Pt/C + TNT-R and Pt/C + TNT-300 were 1.41 and 1.38, respectively, both higher than that of Pt/C + TNT-400 (1.11), illustrating better tolerance of water-containing catalysts to carbonaceous species. Furthermore, a comparison between the I_f/I_b ratios for the two water-containing catalysts reveals that Pt/C + TNT-R had a higher value than Pt/C + TNT-300. This demonstrates that more structural water is favorable for improving the tolerance of the Pt/C + TNT-X catalysts to poisoning species.

In the inset of Fig. 3, it can be clearly seen that the onset potentials (the potential at which $I \geq 25$ mA mg^{-1} Pt) for Pt/C + TNT-R and Pt/C + TNT-300 were much lower than that of Pt/C + TNT-400. To compare them accurately, the precise onset potentials are listed in Table 1, the onset potentials for Pt/C + TNT-R and Pt/C + TNT-300 were at 0.21 and 0.20 V, both of which were about 0.20 V lower than that of Pt/C + TNT-400 (0.40 V). Furthermore, according to the last column of Table 1, there were no significant changes in the BET surface area for the three TNTs. This fact indicates that ethanol oxidation kinetic could apparently be enhanced by reducing the onset potential of ethanol oxidation due to the existence of structural water in TNT-R and TNT-300.

CO stripping test is another method that can directly reflect the tolerance of the catalyst to CO-like poisoning species. Fig. 4 shows the CO stripping curves for Pt/C + TNT-R, Pt/C + TNT-300 and Pt/C + TNT-400. Significant differences in the pre-adsorbed CO oxidation peak potentials were observed. The CO oxidation peak potentials for Pt/C + TNT-R and Pt/C + TNT-300 lay at 0.49 and 0.50 V, lower than 0.59 V for Pt/C + TNT-400 catalysts by 0.10 V. This suggests that the water-containing catalysts could oxidize CO more quickly at lower potential than the catalyst without water, which was helpful for releasing the active sites of the Pt to further oxidize ethanol.

From the above results, we have reason to attribute the increased catalytic activity of Pt/C + TNT-R and Pt/C + TNT-

Table 1
Characteristic data of ethanol oxidation at Pt/C + TNT-R, Pt/C + TNT-300 and Pt/C + TNT-400 electrode and BET area for TNT-R, TNT-300 and TNT-400

Pt/C + TNT	Ethanol electro-oxidation				Specific surface areas (for TNT) (m^2 g^{-1})
	E_{onset}/V	E_{Peak}/V	I_f/I_b ratio		
Treatment temperature (°C)	R	0.21	0.81	1.41	340.12
	300	0.20	0.79	1.38	343.08
	400	0.40	0.82	1.11	345.45

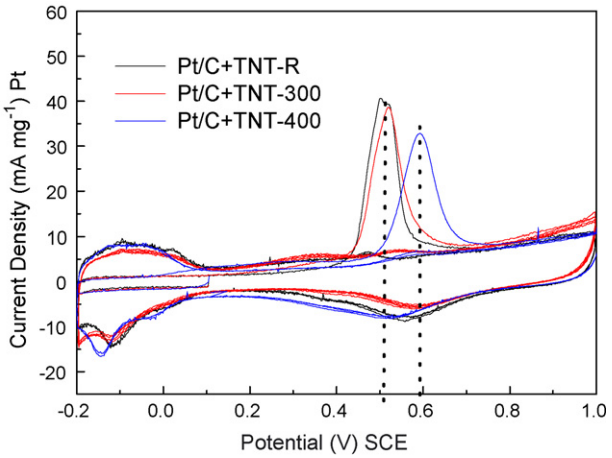

Fig. 4. CO stripping voltammograms in 1 M $HClO_4$ solutions with a scan rate of 10 mV s^{-1}.

300 for ethanol oxidation to the presence of structural water in the TNTs. The inherent TNT–OH bonds on TNT-R and TNT-300 can donate hydroxide species directly to the platinum sites to oxidize CO-like species according to bi-functional mechanism as the way hydrous ruthenium oxide does [26–28], and this would lead to the excellent catalytic activity for ethanol oxidation. In contrast, Pt/C + TNT-400 must activate the H_2O in the electrolyte at a certain potential to form hydroxide species to oxidize the poisoning species for further ethanol oxidation. The assistance of inherent TNT–OH bonds was more apparent at the initial stage of ethanol oxidation.

Fig. 5 shows the chronoamperometric curves on Pt/C + TNT-R, Pt/C + TNT-300 and Pt/C + TNT-400 electrodes in 1 M C_2H_5OH + 1 M $HClO_4$. Prior to the electrochemical endurance test, the working electrodes were pretreated as follows: the potential was stepped up from the open circuit condition to 0.7 V; then 2 s later, it was instantaneously lowered to 0.3 V for 2 s to remove the adsorbed oxides or hydroxides formed on the electrode at 0.7 V. Normal recording of the current transients then proceeded with the potential stepped up to 0.45 V and maintained at that level for 3600 s.

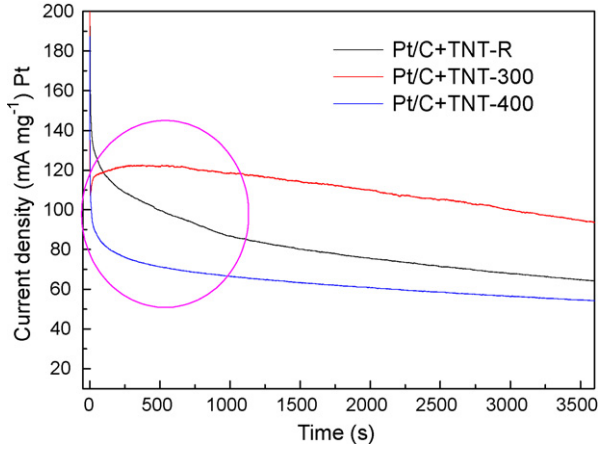

Fig. 5. Current density–time curves at 0.45 V for 3600 s at Pt/C + TNT-R, Pt/C + TNT-300 and Pt/C + TNT-400 electrode in 1 M C_2H_5OH + 1 M $HClO_4$ solutions.

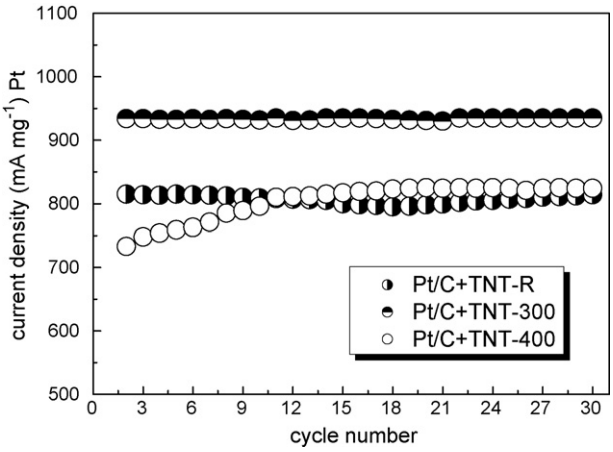

Fig. 6. Peak current density of the first 30 cycles for stability test of Pt/C + TNT-R, Pt/C + TNT-300 and Pt/C + TNT-400 over 250 cycles of ethanol electro-oxidation.

As shown in Fig. 5, the current decay with time could be observed for the three electrodes. The water-containing catalysts had higher current densities at all the time, demonstrating the advantage of the structural water in the TNTs. Between the two water-containing catalysts, Pt/C + TNT-300 had a higher current density than Pt/C + TNT-R. In addition, their decay trends in the current densities were different. At the Pt/C + TNT-R electrode, the current density decay was continuous; whereas at Pt/C + TNT-300 electrode, it ascended at first, and then decayed slowly with time. This may be related to the difference in the amount of structural water in the TNTs. In Pt/C + TNT-R, enough –OH on the TNTs could react directly with the poisoning species produced at the beginning of ethanol oxidation; so that the current density was higher than that of Pt/C + TNT-300 in the first 100 s, even though it decayed quickly with time due to the poor transfer of ethanol in the catalyst layer. On the other hand, in Pt/C + TNT-300, ethanol could occupy the position of the structural water that the TNTs had lost and be supplied to Pt; hence the current density ascended and exceeded that of Pt/C + TNT-R after about 120 s. This result shows that ethanol could be more quickly transferred in the catalyst layer with less structural water, which also led to higher current density of ethanol oxidation on the surface of the catalysts besides bi-functional mechanism.

To understand further the role of structural water in TNTs, the as-prepared electrode catalysts were subjected to a long term repeated scanning of 250 cycles by cyclic voltammograms of ethanol oxidation. The peak current densities (0.80 V vs. SCE) of ethanol oxidation of the first 30 cycles were shown in Fig. 6. It can be observed that the electro-catalytic activities of Pt/C + TNT-R and Pt/C + TNT-300 were more stable than Pt/C + TNT-400; and that their highest peak current densities could be reached more quickly than Pt/C + TNT-400 in the first 15 cycles. This implies that the water-containing catalysts needed a shorter induction period than Pt/C + TNT-400, proving the advantage of the inherent –OH bond on the TNTs in removing the poisoning species. After the first 15 cycles, the current density for Pt/C + TNT-R decreased a little due to the poor transfer of ethanol in the catalyst layer, while that for Pt/C + TNT-300

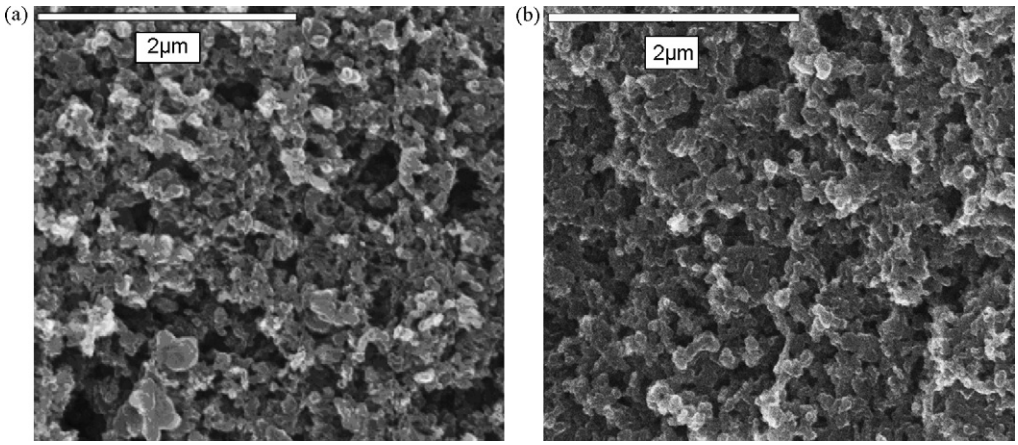

Fig. 7. SEM images for Pt/C + Nafion (a) and Pt/C + TNT-400 + Nafion (b).

remained steady. In addition, we have also observed that the current density at the Pt/C + TNT-300 electrode was higher than that at the Pt/C + TNT-R electrode in all the 250 cycles (not shown). This agreed well with the potentiostatic results in Fig. 5, thus confirming the importance of ethanol transfer in the catalyst layer.

As there is little difference in morphology among Pt/C + TNT-R, Pt/C + TNT-300 and Pt/C + TNT-400, only the SEM images of Pt/C + Nafion and Pt/C + TNT-400 + Nafion are shown in Fig. 7. In Fig. 7a, the morphology of Pt/C appears very loose and there are large amount of voids. The void is about 150 nm in size, and thus can hold the TNTs, which are 8 nm in diameter and 100 nm in length. In Fig. 7b, the morphology of Pt/C + TNT-400 looks very compact and fewer voids can be seen, indicating that the TNTs have entered the voids. The liquid-like morphology among the Pt/C + TNT-400 particles in Fig. 7b shows that the good transfer of Nafion solution in the catalyst layer due to the addition of TNT-400. Since the Nafion solution used in the experiment contained 20% Nafion and 80% ethylene glycol, the smooth transfer of Nafion reflected the smooth transfer of ethylene glycol, and by implication, ethanol. This explains the better catalytic activity of Pt/C + TNT-300 for ethanol electro-oxidation over Pt/C + TNT-R, since the TNTs containing less structural water could probably trap more ethanol and supply it to the adjacent platinum to oxidize quickly.

4. Conclusion

The work presented here confirms our previous report [14] that TNTs could promote Pt/C catalyzing ethanol oxidation due to the existence of structural water. Besides, we further studied the effect of structural water in TNTs on the performance of Pt/C + TNT catalysts in terms of the electrochemical activity of ethanol oxidation by using CV, chronoamperometry and CO stripping voltammetry at 25 °C in acid solutions.

Based on our results, the following conclusions can be drawn: (1) The tolerance of Pt/C catalysts to CO-like poisoning species for ethanol oxidation was enhanced by the TNTs due to the existence of structural water. The results of cyclic voltammetry for ethanol and pre-absorbed CO oxidation showed that the catalyst tolerance increased with the amount of structural water in the TNTs. (2) The induction period of ethanol oxidation was shortened and the stability of the Pt/C + TNT catalysts was improved because of the rapid removal of CO-like poisoning species by the inherent –OH on the TNTs. (3) Even though too much structural water in TNTs could increase CO tolerance, it could also decrease the catalytic activity of Pt/C + TNT catalysts through decelerating the ethanol transfer in the catalyst layer. (4) The optimal catalyst for ethanol oxidation was found to be Pt/C + TNT-300, in which not only the bi-functional mechanism can well work but also ethanol can be easily transferred.

Acknowledgements

The authors appreciate the financial support of the State Key Basic Research Program of PRC (2002CB211803) and the National Natural Science Foundation of China (90410002).

References

[1] H.A. Gasteiger, N. Markovic, P.N. Ross, E.J. Cairns, J. Phys. Chem. 97 (1993) 12020–12029.
[2] W.L. Xu, T.H. Lu, C.P. Liu, W. Xing, J. Phys. Chem. B 110 (2006) 4802–4807.
[3] J. Zhu, Y. Su, F.Y. Cheng, J. Chen, J. Power Sources 166 (2007) 331–336.
[4] J.M. Léger, S. Rousseau, C. Coutanceau, F. Hahn, C. Lamy, Electrochim. Acta 50 (2005) 5118–5125.
[5] D.J. Guo, H.L. Li, J. Power Sources 160 (2006) 44–49.
[6] S. Mukerjee, R.C. Urian, S.J. Lee, E.A. Ticianelli, J. McBreen, J. Electrochem. Soc. 151 (2004) A1094–A1103.
[7] C. Roth, A.J. Papworth, I. Hussain, R.J. Nichols, D.J. Schiffrin, J. Electroanal. Chem. 581 (2005) 79–85.
[8] C. Lu, C. Rice, R.I. Masel, P.K. Babu, P. Waszczuk, H.S. Kim, E. Oldfield, A. Wieckowski, J. Phys. Chem. B 106 (2002) 9581–9589.
[9] Y.X. Bai, J.J. Wu, X.P. Qiu, J.Y. Xi, J.S. Wang, J.F. Li, W.T. Zhu, L.Q. Chen, Appl. Catal. B: Environ. 73 (2007) 144–149.
[10] K.W. Park, S.B. Han, J.M. Lee, Electrochem. Commun. 9 (2007) 1578–1581.
[11] L.H. Jiang, G.Q. Sun, Z.H. Zhou, S.G. Sun, Q. Wang, S.Y. Yan, H.Q. Li, J. Tian, J.S. Guo, B. Zhou, Q. Xin, J. Phys. Chem. B 109 (2005) 8774–8778.
[12] M. Adachi, Y. Murata, M. Harada, Chem. Lett. 8 (2000) 942–944.
[13] M. Wang, D.J. Guo, H.L. Li, J. Electrochem. Soc. 178 (2005) 1996–2000.
[14] H.Q. Song, X.P. Qiu, X.X. Li, F.S. Li, W.T. Zhu, L.Q. Chen, J. Power Sources 170 (2007) 50–54.

[15] J. Hu, J.G. Deng, S.Y. He, Z.G. Chang, J.S. Zhao, J.N. Liu, Chin. Mater. Sci. Eng. 19 (2001) 71–73.
[16] T. Kasuga, M. Hiramatsu, A. Hoson, T. Sekino, K. Niihara, Adv. Mater. 11 (1999) 1307–1311.
[17] T. Kasuga, M. Hiramatsu, A. Hoson, T. Sekino, K. Niihara, Langmuir 14 (1998) 3160–3163.
[18] Y.L. Hsin, K.C. Hwang, C.T. Yeh, J. Am. Chem. Soc. 129 (2007) 9999–10010.
[19] M.C. Gutiérrez, M.J. Hortigu1ela, J.M. Amarílla, R. Jiménez, M.L. Ferrer, F.D. Monte, J. Phys. Chem. C 111 (2007) 5557–5560.
[20] J.C. Huang, Z.l. Liu, C.B. He, L.M. Gan, J. Phys. Chem. B 109 (2005) 16644–16649.
[21] Y.Y. Mu, H.P. Liang, J.S. Hu, L. Jiang, L.J. Wan, J. Phys. Chem. B 109 (2005) 22212–22216.
[22] Z.L. Liu, X.Y. Ling, X.D. Su, J.Y. Lee, J. Phys. Chem. B 108 (2004) 8234–8240.
[23] R. Manohara, J.B. Goodenough, J. Mater. Chem. 2 (1992) 875–884.
[24] F. Vigier, C. Coutanceau, F. Hahn, E.M. Belgsir, C. Lamy, J. Electroanal. Chem. 563 (2004) 81–89.
[25] G.A. Camara, T. Iwasita, J. Electroanal. Chem. 578 (2005) 315–321.
[26] A. Kabbabi, R. Faure, R. Durand, B. Bedan, F. Hahn, J.M. Leger, C. Lamy, J. Electroanal. Chem. 444 (1998) 41–53.
[27] K.E. Swider, C.I. Merzbacher, P.L. Hagans, D.R. Rolison, J. Non-cryst. Solids 225 (1998) 348–352.
[28] D.R. Rolison, P.L. Hagans, K.E. Swider, J.W. Long, Langmuir 15 (1999) 774–779.